

Article

Effect of Thermal Bridges of Different External Wall Types on the Thermal Performance of Residential Building Envelope in a Hot Climate

Hameed Al-Awadi ^{1,*}, Ali Alajmi ¹ and Hosny Abou-Ziyan ^{1,2}

¹ Mechanical Engineering Department, College of Technological Studies, Public Authority for Applied Education and Training, Kuwait City 70554, Kuwait; af.alajmi@paaet.edu.kw (A.A.); hz.abouziyan@paaet.edu.kw (H.A.-Z.)

² Mechanical Power Engineering Department, Faculty of Eng., Helwan University, Cairo 11718, Egypt

* Correspondence: ha.alawadi@paaet.edu.kw; Tel.: +965-9922-6785; Fax: +965-2481-1753

Abstract: In this paper, the thermal performance of residential building envelopes including thermal bridges (TBs) in a hot climate, using four different exterior wall types, is modelled and assessed. TBs at the junctions between columns and walls and between walls and slabs of the ground floor, roof, and intermediate floors are considered. The tested wall types are classical (two layers of cement blocks with insulation in between), autoclaved aerated concrete bearing (AAC-B), AAC column and beam (AAC-CB), and exterior insulation and finish system (EIFS). The results indicated that thermal bridges have a considerable effect and determine the best external wall type which was the EIFS that has a continuous exterior insulation. EIFS proved to reduce the heat transmission with the outdoor environment for residential buildings by 101.8, 51.2, and 13.9% than the AAC-CB, AAC-B, and classical walls, respectively. Thermal bridges effect on the building envelope using the EIFS is insignificant as the thermal resistance of the envelope and wall differs by less than 1% for small areas. The overall heat transfer coefficients for small buildings are larger than those for large buildings by 8–26%. As the number of intermediate floors increases from 1 to 50, the envelope overall heat transfer coefficient increases by 4.5% for the EIFS, 14.1% for classical, and 19.5% for AAC-CB walls. The AAC-CB, as the common practice wall structure in many hot climate countries, has the lowest performance among the tested wall types.

Keywords: wall types; thermal bridges; thermal insulation; building envelope; envelope performance; equivalent resistance



Citation: Al-Awadi, H.; Alajmi, A.; Abou-Ziyan, H. Effect of Thermal Bridges of Different External Wall Types on the Thermal Performance of Residential Building Envelope in a Hot Climate. *Buildings* **2022**, *12*, 312. <https://doi.org/10.3390/buildings12030312>

Academic Editor: Baojie He

Received: 20 January 2022

Accepted: 16 February 2022

Published: 6 March 2022

Publisher's Note: MDPI stays neutral with regard to jurisdictional claims in published maps and institutional affiliations.



Copyright: © 2022 by the authors. Licensee MDPI, Basel, Switzerland. This article is an open access article distributed under the terms and conditions of the Creative Commons Attribution (CC BY) license (<https://creativecommons.org/licenses/by/4.0/>).

1. Introduction

Buildings contribute to environmental pollution substantially as they are responsible for about 36% of worldwide primary energy consumption and 39% of CO₂ emissions [1]. The energy demand of residential buildings is up to 40% [2] on the global level and over 70% in hot climate regions, which is mostly due to active cooling [3].

The building envelope (roof, walls, foundation, windows, and doors) is controlling the amount of heat exchange with the environment, and consequently the building energy consumption [4]. It is claimed that the external wall is responsible for 25–30% of thermal energy transmitted to the building [5]. Thus, the thermal performance of the building envelope is a crucial aspect that needs to be enhanced by designers and building construction firms. This essentially means the thermal bridges (TBs) in which the heat losses bypass the discontinuous insulated layers that may represent 50–80% of an exterior wall (TBs) [6]. TBs occur when there is a break caused by several situations, such as the junctions between the external wall with floor roof, and column, i.e., walls have thermal bridges at the junctions with the concrete columns, concrete slabs between floors, ground floor, roof, etc. One of the

common measures, in enhancing building envelope thermal performance and reducing greenhouse gas emissions, is increasing the insulation thickness [7].

Many studies assess the benefits of increasing the insulation thickness of walls and roofs on energy reduction such as the work done by Radhi [8], where the increase of insulation thickness reduces the consumption under different climate conditions by 17.4–23.8%. In another study by the same author, two-building envelopes, made from an autoclaved aerated concrete (AAC) and cement block, were compared and showed a saving of 7% by the AAC residential building over the business-as-usual wall layer (cement block) [9]. Other studies have investigated the insulation type [10–12], thickness [10,13–15], and location [16]. However, those studies did not consider the effect of thermal bridges on the building envelope performance and energy consumption.

On the other hand, many standards and codes, such as ISO 14683 [17], have suggested simplified methods to include TB contribution. Several recent studies consider the effect of the thermal bridge on the external wall of residential buildings. For instance, Friess et al. [18] experimentally assessed residential villas in Dubai and reported that up to 53% of their external walls were uninsulated. The authors [18] studied the effect of TB on a mid-plane insulation block, which showed less efficiency than the external insulation block by 22.9%. Hua and Fuad [19] reported a 38–42% increase in the heating demand due to the thermal bridges between floors of high-rise residential buildings for several studied cities. In another study by the authors for a low-rise building in Canada, the effect of thermal bridge using 2D/3D dynamic method is more than that using the simplified method (equivalent U-value) by 8–13% [20]. Martin et al. [21] studied the effect of the thermal bridge on high-rise residential buildings of double-wall construction and reported an increase in the heating demand by 10.3% in a cold climate. An analysis of timber frame wall thermal bridges showed a different overall heat transfer coefficient (U) than the specified value by the timber panel manufacture [22]. Most of the research was not specifying the value of the thermal bridge resistance, however, it is usually given as a percentage value [23].

The above literature review indicates that the effect of the thermal bridge depends on the type of wall structure including brick type, wall thickness, and insulation location and thickness. However, the previous studies focus either on the thermal bridges between floors of high-rise buildings or thermal bridge locations for only one wall type structure. There are many types of envelope structures that range from lightweight to heavy-weight walls. The previous work lacks the accurate effect of different external wall structures on the thermal bridges and envelope performance, particularly in hot climates. Thus, it makes it difficult to select the suitable wall type that has the best thermal performance of the building envelope. In addition, a multi-dimensional heat transfer analysis of thermal bridges received less attention from researchers and practitioners on low-rise residential buildings [24,25].

This paper investigates the effects of four different wall structures on the thermal bridges and the building envelope performance, in a hot climate, using two-dimensional mathematical models. The tested wall types are classical (cement blocks with insulation in between), autoclaved aerated concrete bearing (AAC-B), AAC column and beam (AAC-CB), and exterior insulation and finish system (EIFS). These wall types are tested with similar concrete columns and slabs to explicitly explore the effect of each wall type. The novelty of this work is identifying the best wall structure type by the comparison of the four wall construction envelopes regarding the overall thermal performance of the building envelopes including the thermal bridges on the four different locations, using two-dimensional heat transfer models.

2. Materials and Methods

2.1. Materials

Figure 1 shows a sample of a building envelope with the four considered thermal bridge locations at the wall junctions with the roof (a), intermediate floor slab (b), slab-on-grade (c), and concrete columns (d). The effect of those thermal bridges on the total

resistance of the building envelope made of four different external wall structures is investigated. Those wall types are the two layers of cement blocks with insulation in between (classical), autoclaved aerated concrete bearing (AAC-B), AAC column and beam (AAC-CB), and exterior insulation and finish system (EIFS). The layer structure and dimensions of each wall type are different from the others. Table 1 lists the details of the four considered external walls and the different concrete slabs. The external wall total resistances range from 1.225 to 1.883 m²K/W and thermal diffusivities from 3.23 to 7.24 × 10⁻⁷ m²/s. While the classical wall has a thermal insulation layer in between, the EIFS has it on the external layer before the cement plaster.

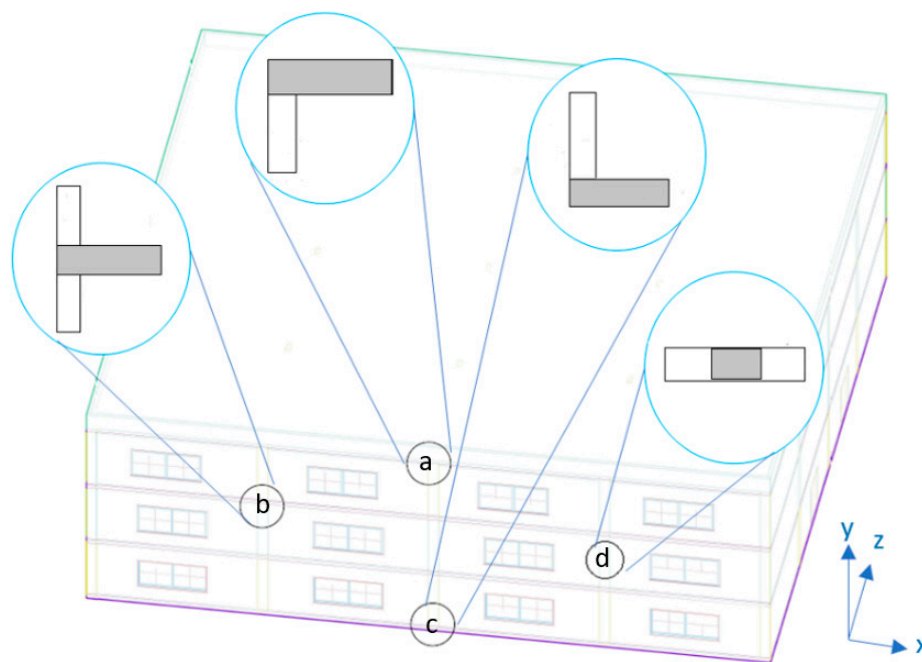


Figure 1. Location of the thermal bridges and the typical layout: (a) roof, (b) intermediate floor slab, (c) slab-on-grade, and (d) concrete column.

Combining the considered four thermal bridges and four wall types produces a total of 15 studied cases, as shown in Figure 2. It is to be noted that the AAC-B is used for low-rise buildings without the use of reinforced concrete columns. In addition, the effect of insulation location and thickness is investigated using the EIFS wall type where two thicknesses (2.5 and 5 cm) of Styropor insulation are examined when installed in the internal or external layer of the wall (next to the cement plaster). To explore the effect of wall type explicitly, the same structure of the concrete slabs and columns is used for all wall types. The listed properties of the walls and slabs (Table 1) are used to determine the characteristics of the considered thermal bridges. In each case, the materials are assumed to be perfectly joined, without cement, and the vapor barriers are not modeled. Contact resistances between materials usually exist; however, the contact resistances are expected to be similar for the four considered building envelopes. Therefore, this assumption is given to focus on the comparison between the wall types without additional offset values of contact resistance.

2.2. Thermal Bridge Modeling Method

2.2.1. Mathematical Model

The governing equation solved in each computational cell is the conservation of energy in two-dimensional form for constant material properties without heat generation:

$$\frac{\partial^2 T}{\partial x^2} + \frac{\partial^2 T}{\partial y^2} = \frac{1}{a} \frac{\partial T}{\partial t} \quad (1)$$

T is the temperature, t is the time, a is the thermal diffusivity of the material, x , and y are the Cartesian coordinate axis, as defined in Figure 1. Under steady state conditions, the above equation becomes:

$$\frac{\partial^2 T}{\partial x^2} + \frac{\partial^2 T}{\partial y^2} = 0 \quad (2)$$

Table 1. Characteristics of the residential building envelope components (walls, slabs, and columns).

Construction	No.	Material	x cm	c_p J/kgK	ρ kg/m ³	k W/mK	R m ² K/W	R_{ca} m ² K/W	U W/m ² K	$a \times 10^{-7}$ m ² /s
Roof slab (1)	1	Sand screed (OL)	7.0	650	2000	1.40	0.050	2.2573	0.430	7.827
	2	PolyFoam	5.0	4470	8.0	0.04	1.250			
	3	Water proofing	0.4	1000	1700	0.50	0.008			
	4	Screed	2.0	650	2000	1.40	0.0143			
	5	Foam concrete	7.0	920	400	0.08	0.875			
	6	Reinforced Concrete slab (IL)	15.0	1000	2400	2.50	0.060			
Slab-on-Grade (2a)	7	Ceramic (IL)	1.0	850	1700	0.80	0.0125	0.1275	7.843	10.000
	8	Tile fix	0.2	630	1.75	0.515	0.0039			
	9	Screed	7.0	650	2000	1.40	0.050			
	10	Reinforced Concrete slab 1% steel (OL)	15.0	1000	2300	2.30	0.065			
Intermediate Floor slab (2b)	11	Ceramic (IL)	1.0	850	1700	0.80	0.0125	0.1225	8.163	10.001
	12	Tile fix	0.2	630	1.75	0.515	0.0039			
	13	Screed	7.0	650	2000	1.40	0.050			
	14	Reinforced Concrete slab (OL)	15.0	1000	2400	2.50	0.060			
External Wall: Classical (4)	a	Cement plaster (IL)	3.0	840	1680	0.82	0.0366	1.836	0.5447	4.981
	b	Cement block	10.0	840	1760	0.66	0.152			
	c	Insulation	5.0	1400	35.0	0.034	1.471			
	d	Cement block	10.0	840	1760	0.66	0.152			
	e	Cement plaster (OL)	2.0	840	1680	0.82	0.0244			
External Wall: AAC Colm. Beam (5) (AAC-CB)	f	Cement plaster (OL)	2.0	840	1680	0.82	0.0244	1.2250	0.8164	3.985
	g	Mesh (Galv. Steel)	0.2	480	7800	12.50	0.00016			
	h	AAC block	20.0	879	600	0.17	1.176			
External Wall: AAC-Bearing (6) (AAC-B)	i	Cement plaster (IL)	2.0	840	1680	0.82	0.0244	1.8826	0.5312	3.223
	j	Plaster Int. —Light Weight (IL)	1.0	879	600	0.17	0.0588			
	k	AAC block—ACICO	30.0	879	600	0.17	1.765			
External Wall: Exterior Insulation and Finish (7) System (EIFS)	l	Plaster Ext. —Light Weight (OL)	1.0	879	600	0.17	0.0588	1.759	0.5685	7.236
	m	Cement plaster (IL)	3.0	840	1680	0.82	0.0366			
	n	Cement block	15.0	840	1760	0.66	0.227			
	o	Insulation (Styropor)	5.0	1400	18.0	0.034	1.471			
Concrete Columns	p	Cement plaster (OL)	2.0	840	1680	0.82	0.0244	0.200	5.000	10.400
	q	Reinforced Concrete slab	50.0	1000	2400	2.50	0.200			

The thermal bridge simulation includes steady-state and dynamic simulations where the steady-state analysis determines the stationary characteristics of the thermal bridges such as the thermal bridge total heat capacity C (Equation (3)) and the thermal resistance R

(Equation (4)) under the standard boundary conditions used for thermal bridge simulation (EN ISO 10211 [26]). The standard boundary conditions are the referenced temperatures $T_e = 1$, $T_{in} = 0$ °C, $h_e = 23$, and $h_{in} = 8$ W/m² K.

$$C = \int_V \rho c dV \quad (3)$$

$$R = \Delta T / q \quad (4)$$

where the heat flux (q) is determined using Equation (5) with ∇T being the tangential gradient operator of the temperature.

$$q = -k \nabla T \quad (5)$$

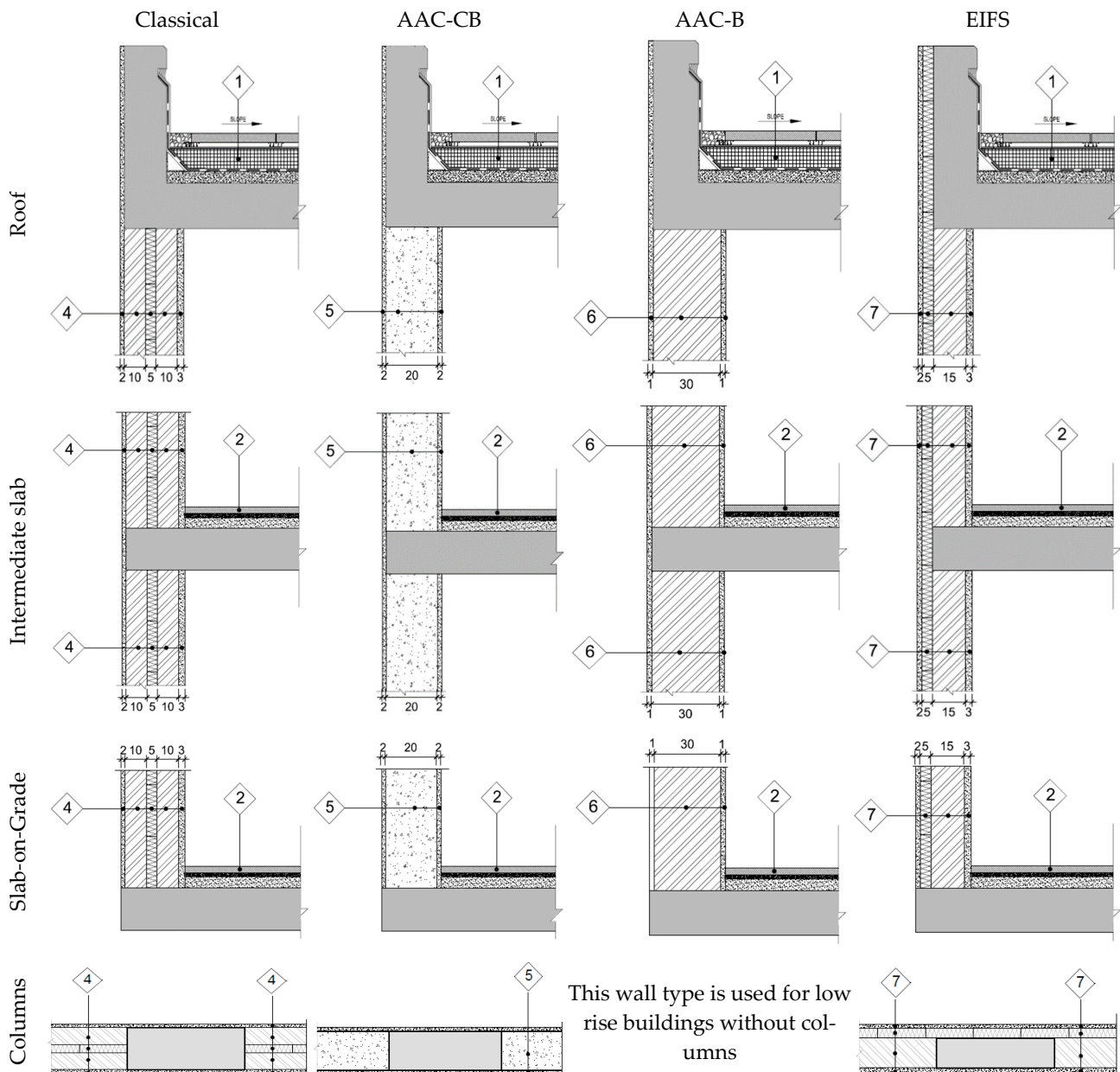


Figure 2. The considered four thermal bridge junctions (roof, intermediate slab, slab-on-grade, and concrete columns) for the tested four wall types. 1. Roof slab; 2a. Slab-on-Grade; 2b. Intermediate Floor slab; 4. Classical; 5. AAC Colm. Beam (AAC-CB); 6. AAC-Block (AAC-B); 7. Exterior Insulation and Finish System (EIFS).

On the other hand, the dynamic simulation is performed to determine the amplitude A_i (24 h) and time lag α_i (24 h) of the heat fluxes through the inner surface based on a 24 h period. The dynamic simulation is conducted under the same standard boundary conditions, except that T_e is replaced by: $T_e = \sin(2\pi t/86400)$. The dynamic simulation is performed for 10 days, and the results were analyzed after seven days (168 h). Quinten and Feldheim [27,28] recommended that the program should run a few days before you can attain an accurate response of the thermal bridges that is independent of the initial conditions of the thermal bridges.

2.2.2. Computational Domain and Mesh Sensitivity Analysis

The computational domain of each of the fifteen thermal bridges shown in Figure 2 is determined by the cut-off planes. They are assumed to be adiabatic planes if they are placed sufficiently far from the 2-D perturbation of the thermal bridges. The cut-off planes are first placed in areas of 1-D heat flow, at one meter from the 2-D detail as recommended by EN ISO 10211 [26] unless there is a closer symmetry plane. Then, the new creating cut-off planes are determined when the inner or outer surface temperatures (T_{si} or T_{se}) between two consecutive planes at the extended boundaries are examined for deviations smaller than 0.01 °C. This indicates that the heat flow in the cut-off planes may be approximated as 1-D with an insignificant effect on the studied computational domain. This avoids unnecessary additional computations of the model and saves computer CPU time and effort.

The fifteen thermal bridge cases shown in Figure 2 are configured, modeled, and tested using fifteen 2-D numerical models. The models are performed using the COMSOL Multiphysics software [29], which is a finite element analysis, solver, and simulation software.

Accurate CFD results require a numerical mesh that is sufficiently refined so that the results obtained do not depend on the mesh used. Therefore, the thermal bridge was meshed with four different resolutions to check for mesh independence and to select the best mesh that gave a converged solution, accurate results, and a reasonable computational time. Coarse (6629 elements), normal (7506 elements), fine (7674 elements), and finer (8997 elements) mesh settings that are self-generated, by the program, have been tested with the simulation models. Table 2 lists the values of inside temperature and heat flux predicted by the different mesh types. In addition, the percentage difference between the predicted values by each mesh relative to that obtained by the finer one is listed in Table 2. Generally, as the mesh size increases, the difference between the predicted value for each mesh and the value for the finer mesh decreased. The difference of stationary temperature and heat flux is lower than 0.01% between the fine and finer meshes. Thus, the sensitivity analysis confirmed the accurate results of the simulations and their independence on mesh size using the fine size mesh.

Table 2. Mesh independence analysis for the thermal bridge of intermediate floors under the standard conditions.

Mesh Type (# Elements)	Coarse (6629)	Normal (7506)	Fine (7674)	Finer (8997)
T_{in} (°C)	0.082459	0.082451	0.082450	0.082447
%Difference	0.014555	0.004852	0.003639	0.0
q_{in} (W/m ²)	0.68169	0.68169	0.68160	0.68162
%Difference	0.01027	0.01027	0.002934	0.0

2.2.3. Validation and Accuracy of the Simulation Model

The model validation is carried out by comparing the numerical results obtained from the present model and the published data of Quinten and Feldheim [27] for the case of thermal bridge of the intermediate floors, under the same boundary conditions. Table 3 lists the predicted and published data [27] of the heat capacity, thermal resistance, and heat flux of the thermal bridge. Using the fine numerical mesh, the difference between the predicted and published data is 0.22% for the heat capacity, 2.17% for the thermal resistance, and

2.21% for the heat flux. Therefore, the results proved that the model is sufficiently accurate to evaluate the characteristics of the thermal bridges.

Table 3. The published and predicted heat capacity (C), thermal resistance (R), and heat flux (q) for the thermal bridge of the intermediate floors.

Case	C (J/m ² K)	R (m ² K/W)	q (W/m ²)
Quinten and Feldheim [27]	608,930	6.49800	0.150560
Present model	610,291	6.64187	0.153894
% Difference	0.22	2.17	2.21

2.3. Assembly Resistance of the Building Envelope

In this paper, an assembly resistance concept is applied to assess the building envelope effectiveness to facilitate the comparison between the different wall structures considered in this work. The thermal resistance (per unit area) of each building envelope component (R_{ca}) is connected in a series of its layers as given in Table 1 for walls, roof, middle slab, and slab-on-grade and in Table 4 for the considered thermal bridges. The total thermal resistance of each (R_c) envelope element can be obtained using the thermal resistance per unit area (R_{ca}) and the area of the component (A_c) as defined in Equation (6).

$$R_c = R_{ca} \times A_c \quad (6)$$

Table 4. The stationary and dynamic characteristics of the thermal bridges (obtained at standard temperature).

Thermal Bridge	Case	C kJ/m ² K	R_{ca} m ² K/W	$\alpha \times 10^7$ m ² /s	S_i m ²	S_e m ²	T_e °C	T_i °C	q_i W/m ²	A_i W/m ²	a_i h
Between floors F	Classical	583.65	0.663	7.742	1.726	0.664	0.934	0.162	1.509	0.548	6.00
	AAC Column Beam	483.70	0.698	7.055	1.869	0.845	0.938	0.154	1.432	0.570	4.75
	AAC bearing	470.54	0.850	6.898	1.645	0.645	0.948	0.122	1.176	0.410	7.00
	EIFS	690.82	1.667	8.315	2.326	1.182	0.974	0.071	0.600	0.110	5.00
Roof Γ	Classical	647.59	0.947	7.5516	1.081	1.745	0.972	0.132	1.056	0.041	8.00
	AAC Column Beam	585.35	0.933	7.6259	1.241	1.847	0.969	0.134	1.072	0.064	5.75
	AAC bearing	547.98	1.054	7.5358	0.987	1.671	0.976	0.119	0.949	0.029	8.50
	EIFS	594.09	1.762	7.8273	1.151	1.765	0.984	0.071	0.568	0.019	7.00
Ground floor L	Classical	653.17	1.729	7.1197	1.278	0.790	0.766	0.009	0.578	0.068	7.75
	AAC Column Beam	445.80	1.516	7.45	1.046	0.525	0.870	0.020	0.660	0.162	5.25
	AAC bearing	467.28	2.234	6.47	1.085	0.605	0.911	0.008	0.448	0.061	8.00
	EIFS	447.99	1.573	6.75	0.998	0.805	0.948	0.011	0.636	0.085	5.50
Column-wall	Classical	784.39	0.844	6.01	1.80	1.80	0.744	0.040	1.185	0.315	5.75
	AAC Column Beam	402.42	0.540	6.24	1.27	1.27	0.780	0.104	1.851	0.827	4.25
	EIFS	532.81	1.622	8.56	1.50	1.50	0.962	0.018	0.617	0.148	5.00

The equivalent resistance of the ground ($R_{eq,g}$), intermediate ($R_{eq,i}$), and last ($R_{eq,l}$) floors can be obtained using Equations (7)–(9), respectively.

$$\frac{1}{R_{eq,g}} = \frac{1}{R_{sg}} + \frac{1}{R_{cg}} + \frac{1}{R_{wg}} + \frac{1}{2R_{si}} \quad (7)$$

$$\frac{1}{R_{eq,i}} = \frac{1}{R_{ci}} + \frac{1}{R_{wi}} + \frac{1}{R_{si}} \quad (8)$$

$$\frac{1}{R_{eq,l}} = \frac{1}{R_{cl}} + \frac{1}{R_{wl}} + \frac{1}{R_{sl}} + \frac{1}{R_r} + \frac{1}{2R_{si}} \quad (9)$$

Figure 3 shows the elevation of the building envelope with the locations of the various resistances used in Equations (7)–(9). R_{cg} , R_{ci} , and R_{cl} are the resistances of the ground,

intermediate, and last floors, respectively. In addition, R_{wlg} , R_{wli} , and R_{wll} are the wall resistance of the ground, intermediate, and last floors, respectively. R_{sg} , R_{si} , and R_{sl} are the resistances of the slab thermal bridges of the ground, intermediate, and last floors, respectively. R_r is the resistance of the roof slab area that is not affected by the roof thermal bridge.

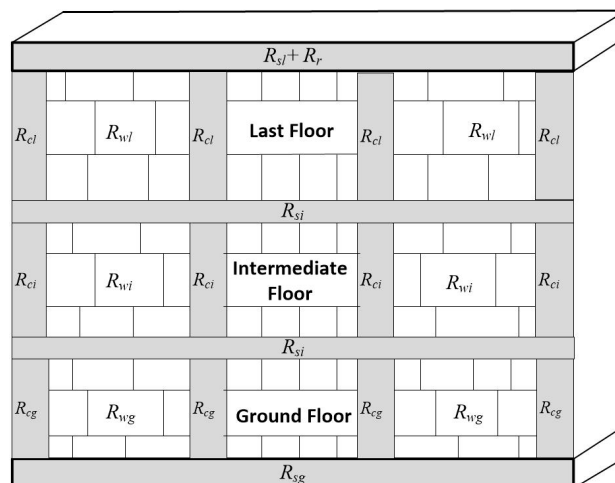


Figure 3. Illustration of the locations of the thermal resistances used in Equations (7)–(9) for the tested building envelope.

The total thermal resistance of the building (R_t) can be obtained for N number of intermediate floors using the parallel resistance concept as follows:

$$\frac{1}{R_t} = \frac{1}{R_{eq,g}} + \frac{N}{R_{eq,i}} + \frac{1}{R_{eq,l}} \quad (10)$$

The overall heat transfer coefficient (U) can be obtained as defined by Equation (11).

$$U = \frac{1}{AR} \quad (11)$$

where A is the area and R is the thermal resistance of the floor or the whole building. The performance of the building envelope may be assessed using either the total thermal resistance or the overall heat transfer coefficient.

3. Results and Discussion

The effects of the four main thermal bridges, in the building envelope, on the four external wall types, are tested. The primary aim is to identify the best-performing wall types among the classical, autoclaved aerated concrete bearing (AAC-B) for low-rise buildings, AAC column and beam (AAC-CB), and exterior insulation and finish system (EIFS) walls. Table 1 indicates that the classical and AAC-B walls have the largest thermal resistance, followed by the EIFS while the AAC-CB wall has the lowest resistance. Accordingly, if the thermal bridge effect is neglected, the building constructed using AAC-B wall will have the best performance and those with AAC-CB wall have the lowest performance. As the area of the thermal bridge may be as large as 50–80% [6] of the external walls, it has a substantial effect on the various types of external walls used in hot climates. Thus, the combined effect of the wall and thermal bridge zones are considered.

In the following sections, the effect of the external wall structures on the thermal bridges is discussed under standard (0 for the air inside the building and 1 for the outside ambient air) and real temperature (shown in Figure 4) conditions. Then, the effect of insulation thickness and location is determined. Finally, the thermal characteristics of the considered four building envelopes are examined to identify the best wall structure.

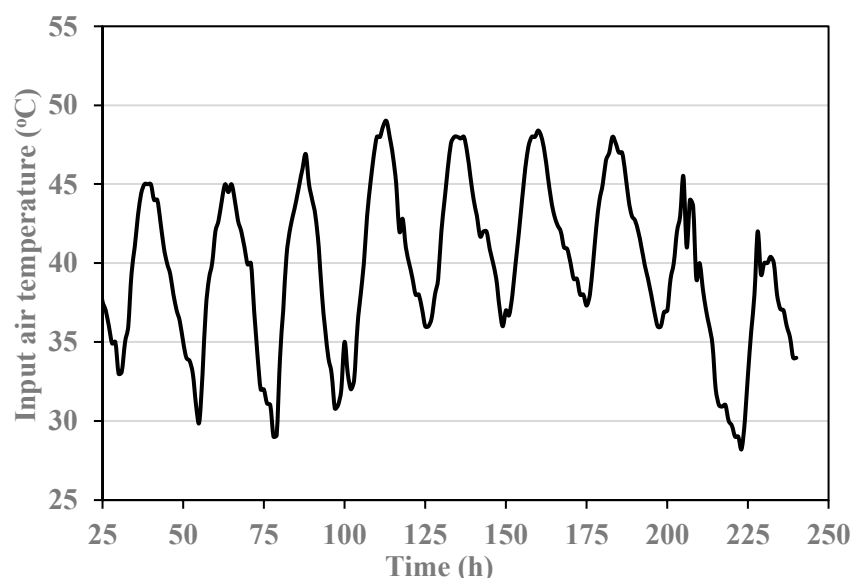


Figure 4. The ten-days input air temperature variations were used to test the various thermal bridges under hot climate conditions.

3.1. Effect of External Wall Structure on the Thermal Bridges

The effect of external wall structure on common thermal bridges in four places such as the junction of the external wall with the concrete slabs between floors, with the roof, and with the ground floor, and the junction between columns and wall is discussed for the four external wall structures. To explore the effect of external wall structure on each of those thermal bridges, the same structure of each concrete slab used in the intermediate floor, roof, ground floor, or columns is used with the various wall types.

In this section, the characteristics of the thermal bridges of the four wall types are obtained and the response of the thermal bridges under hot climate conditions is discussed. Among the thermal bridge characteristics are the temperature amplitude and time lag. The temperature amplitude is the difference between the highest and lowest indoor or outdoor temperatures over a certain period (one day). There are different approaches to obtain time lag; in this study, it is measured as the interval of time between a certain peak or valley of the outdoor temperature and the corresponding peak or valley of the indoor temperature.

3.1.1. Characteristics of the Thermal Bridges

As discussed in Section 2, the thermal bridge characteristics are determined under the standard temperature conditions (0 for the air inside the building and 1 for the outside ambient air). Table 4 lists the essential characteristics of the four thermal bridge types for the different wall structures. It is to be noted that the case of column-wall has three wall structures as the AAC-B wall has no columns. Since the inner and external areas of the thermal bridges are different for each wall structure and different from one thermal bridge to another, the order of thermal resistance, thermal diffusivity, time lag, and heat capacity is different for each type of thermal bridge. In general, the orders of inlet temperature, inside heat flux, and the inside heat flux amplitude (A_i) are in the reverse order of the resistances of the thermal bridges. This indicates the inverse relation between those parameters and the thermal resistance according to Fourier's law of conduction. However, the order of time lags depends on the thermal diffusivity, heat capacity per unit area, thickness, and geometry of the thermal bridge. The low thermal diffusivity of the thermal bridges means a slow transfer of heat through the thermal bridge and thus a large time lag. On the other hand, a small thermal resistance means large heat transfers to the building and consequently a large cooling load.

For the intermediate thermal bridges between floors, Table 4 indicated that the AAC-B and AAC-CB walls have relatively low thermal resistance, thermal diffusivity, and heat

capacity compared to the EIFS. However, the maximum variations of the thermal resistance, heat capacity, and thermal diffusivity between the various wall structures are about 60%, 32%, and 17%, respectively, which implies the order of their importance. In addition, the large heat capacity and thermal resistance of the EIFS enhances its capability of the temperature attenuation of the thermal bridge as it decreases the inside wall temperature to 0.071 °C compared to 0.162 °C for the classical wall. The steady-state characteristics showed that the inside heat flux of the thermal bridge of the EIFS is lower than those of the other walls by 60.2% for the classical wall, 58.1% for the AAC-CB wall, and 49.0% for the AAC-B wall. On the other hand, the harmonic analysis showed that the heat flux amplitude for the thermal bridges of the EIFS is less than half that of the classical and AAC-CB walls. The time lag of the thermal bridges using the EIFS is lower than that using classical wall by 1 h and AAC-B wall by 2 h and higher than that of AAC-CB by 0.25 h. Again, this is a manifestation of the thermal bridge characteristics (C , R , a ; Table 4) of the different types of structures.

The data of thermal bridges of the roof (Table 4) revealed that the EIFS has the largest thermal resistance and thermal diffusivity with reasonable heat capacity. The variations in the thermal resistance, heat capacity, and thermal diffusivity between the various wall types are about 47.1%, 15.4%, and 3.7%. Again, the variation of the thermal diffusivity is very limited. Thus, the steady-state analysis indicated that the EIFS offers heat flux and temperature attenuation better than the other wall types by 40.1–47.0%. This is due to its relatively larger thermal resistance compared to the other wall structures. On the other hand, the harmonic analysis revealed that the heat flux amplitude of the EIFS is less than half that of the classical wall and one-third that of the AAC-CB. In addition, the time shift of the EIFS is greater than that of the AAC-CB by over one hour and less than those of the classical and AAC-B walls by 60 and 90 min, respectively. This reflects the effect of the thermal diffusivity, heat capacity, and thermal resistance on the dynamic response of the roof thermal bridges.

The thermal bridges of the ground floor are exceptional to the other cases as the AAC-B wall has the largest thermal resistance and the lowest thermal diffusivity and the classical wall has the largest heat capacity among the walls (Table 4). Thus, the AAC-B attains the lowest inside wall temperature, heat flux, heat flux amplitude, and largest time constant. In addition, it attains a larger time lag than the other tested wall structures. This is mainly attributed to the thermal resistance characteristics and the conditions of the building foundation.

The effect of reinforced concrete column thermal bridges on the various wall structures is described in the last part of Table 4. The thermal resistance of the EIFS is almost double the classical wall and triple the AAC-CB wall. Accordingly, the heat flux of the EIFS is about half that of the classical wall and one-third that of the AAC-CB wall. In addition, the EIFS provides the lowest inside wall temperature and heat flux amplitude. The time lag of the EIFS is larger than the AAC-CB and lower than the classical wall by about 45 min.

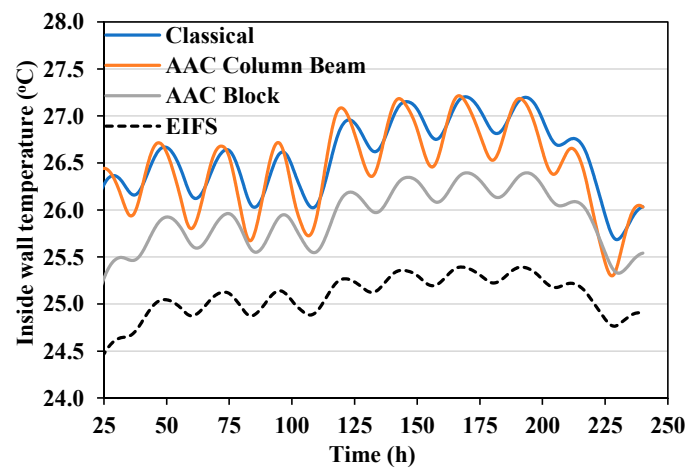
In conclusion, the EIFS provides the largest resistance and lowest heat flux for the thermal bridges, except for the thermal bridge of the ground floor where the AAC-B yields the largest thermal resistance. On the other hand, the AAC-CB offers the lowest resistance and largest heat flux for thermal bridges of the roof, ground floor, and column-wall, except for the thermal bridge between floors where the classical wall structure yields the lowest thermal resistance and largest heat flux. In addition, the largest time lag takes place using the AAC-B and classical wall structures whereas the EIFS and AAC-CB yield relatively lower time lag. In evaluating the thermal bridges, the large thermal resistance and low heat flux are preferred over the large time lag. Thus, the EIFS and the AAC-B have a distinct advantage over the classical and AAC-CB wall structures.

3.1.2. Response of Thermal Bridges under Hot Climate Conditions

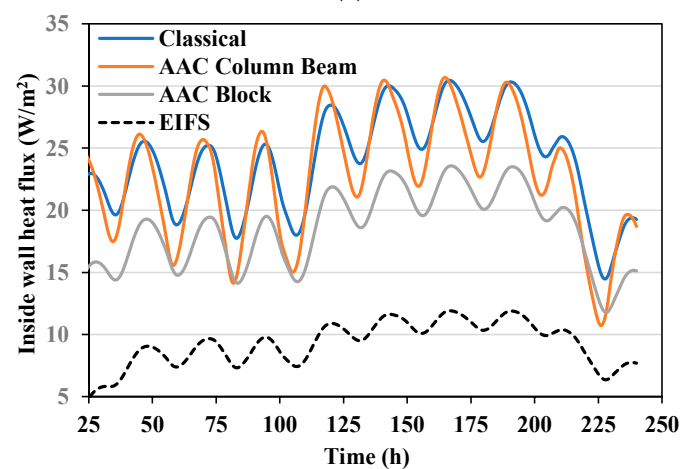
The characteristics of the thermal bridges are obtained under the standard temperatures. Then, the response of thermal bridges is obtained under the actual weather conditions

of hot climate countries. Figure 4 shows the input air temperature used to test the thermal bridges of the various tested walls. The input temperature fluctuates between a maximum value of 48 °C and a minimum value of 28.43 °C with a temperature amplitude of about 19.57 °C. Previous studies [27,28] recommended that the simulation program should run a few days before you can attain an accurate response of the thermal bridges that avoid the effect of the initial conditions, of the thermal bridges, on their response. Thus, the thermal bridges are tested for ten days (240 h), and their responses are shown after 24 h from the starting of the run to avoid the effect of initial conditions of the thermal bridges.

Figure 5a shows the inside wall temperature response of the thermal bridge of intermediate floors using the four tested walls. The AAC-CB and the classical walls yield large and comparable inside wall temperatures whereas the EIFS attains the lowest inside wall temperature. The maximum temperatures are damped from 48 °C to 28.9, 27.2, 26.4, and 25.4 °C for classical, AAC-CB, AAC-B, and EIFS, respectively, i.e., the temperature damping ranges from 19.1 to 22.6 °C. The corresponding average temperatures of the listed walls are 27.9, 26.5, 25.9, and 25.1 °C with temperature amplitudes of 2.46, 1.92, 1.12, and 0.91 °C, respectively. Thus, the temperature amplitude is reduced from 19.57 °C for the outdoor air temperature to 0.91–2.46 °C for the tested thermal bridges. In addition, the time lag is calculated, from the peak of inlet air temperature at time 88 h, to be 10.50, 9.50, 9.00, and 7.50 h for AAC-B, classical, EIFS, and AAC-CB walls. However, the time lag of the same walls, based on the first valley of inlet air temperature at 55 h, is 7.00, 6.00, 5.00, and 4.75 h. Usually, the time lag is reported based on the valley, not the peak [30].



(a)

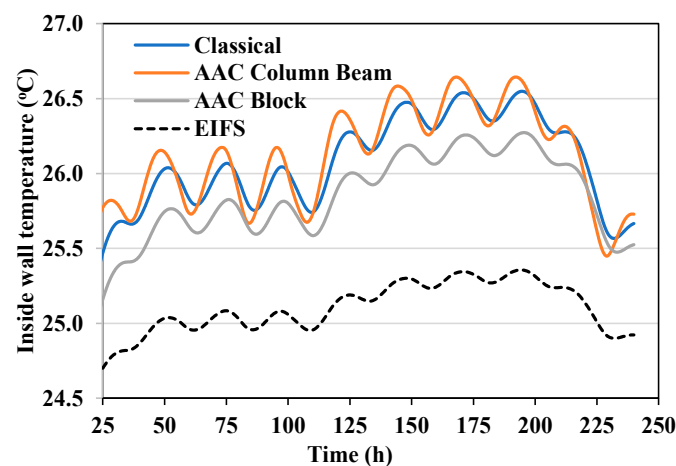


(b)

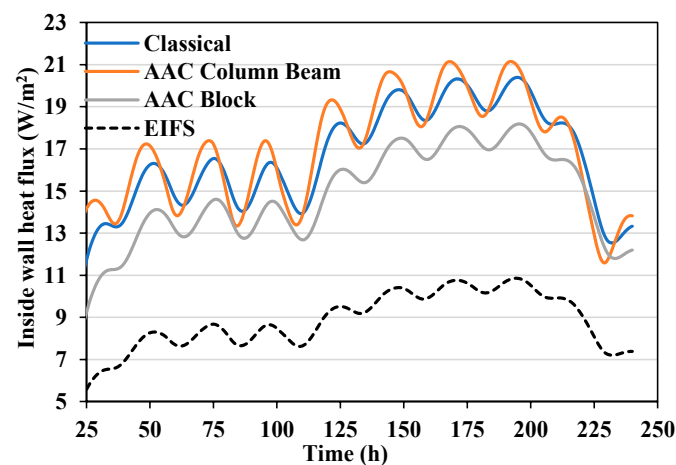
Figure 5. Inside wall temperature and heat flux of the thermal bridges of the intermediate floors using tested four walls. (a) inside wall temperature, (b) inside heat flux.

Figure 5b illustrates the inside wall heat flux fluctuations of the thermal bridge between floors using the four tested walls for the same period (from 25 to 240 h) as in Figure 5a. The pattern of the inside heat flux follows that of the inside wall temperature of the thermal bridges of all wall types. The average heat flux is 35.2, 22.76, 18.60, and 9.28 W/m², with corresponding heat flux amplitude of 12.17, 9.98, 5.89, and 3.52 W/m² for the classical, AAC-CB, AAC-B, and EIFS walls, respectively. Clearly, the EIFS achieves the best performance among the tested thermal bridges. The order of the static and dynamic responses of the thermal bridges between floors is mainly attributed to their characteristics (Table 4) as discussed earlier in Section 3.1.1.

Figure 6a shows the inside wall temperature of the roof thermal bridge of the various wall structures. The average inside wall temperatures of the classical, AAC-CB, AAC-B, and EIFS walls are 26.64, 26.09, 26.27, and 25.36 °C with temperature amplitudes of 1.05, 1.20, 1.09, and 0.64 °C, respectively. The maximum temperatures are damped from 48 °C to 26.6, 26.1, 26.3, and 25.4 °C for classical, AAC-CB, AAC-B, and EIFS, respectively, i.e., the maximum temperature is damped by 21.4–22.6 °C. The corresponding time lags, based on the first temperature valley, of the listed walls, are 8.5, 5.75, 8.5, and 7.0 h. It is observed that the EIFS still provides the best performance, in terms of the average wall temperature and temperature amplitudes, among the tested wall structures. This is due to its large thermal resistance and thermal diffusivity.



(a)

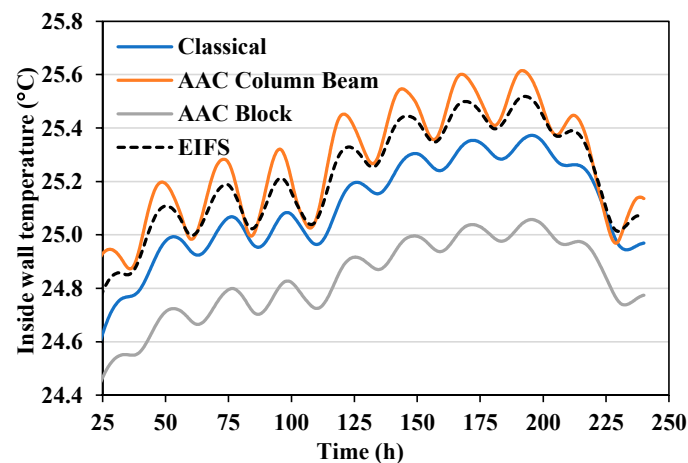


(b)

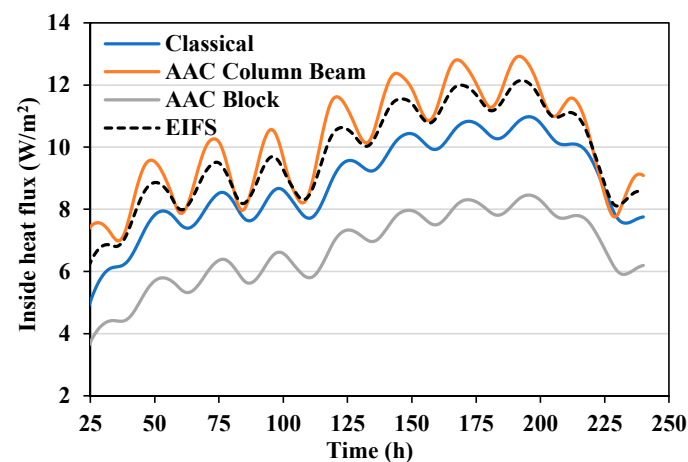
Figure 6. Inside wall temperature and heat flux of the thermal bridges of the roof using tested four walls. (a) inside wall temperature, (b) inside heat flux.

On the other hand, the inside wall heat flux of the roof thermal bridges is illustrated in Figure 6b. The average heat flux of the classical, AAC-CB, AAC-B, and EIFS walls are 16.69, 16.98, 14.88, and 8.88 W/m² with heat flux amplitudes of 4.21, 4.78, 4.36, and 2.58 W/m², respectively. Again, the relatively large thermal resistance causes the EIFS wall to provide superior temperature damping, with low-temperature amplitude, heat flux, and heat flux amplitude among the tested wall structures.

The response of the various wall structures of the ground floor thermal bridges is depicted in Figure 7a,b. In this case, the AAC-B wall provides the best performance followed by the classical, EIFS, and AAC-CB walls. This is evident in terms of the inside wall temperature (Figure 7a) and heat flux (Figure 7b). The average temperature of the classical, AAC-CB, AAC-B, and EIFS walls are 25.1, 25.3, 24.8, and 25.2 °C with temperature amplitudes of 0.73, 0.74, 0.58, and 0.72 °C, respectively. The temperature damped from 48 °C to 25.4, 25.6, 25.1, and 25.5 °C for the classical, AAC-CB, AAC-B, and EIFS walls, respectively. That is, the inlet air temperature is damped by an average value of 22.65 °C (22.4–22.9 °C). The time lags (based on the minimum temperature valley) for the listed walls are 5.50, 7.75, 8.25, and 5.50 h. On the other hand, Figure 7b shows that the average inside heat flux of the classical, AAC-CB, AAC-B, and EIFS walls are 8.88, 10.19, 6.71, and 9.79 W/m² with inside heat flux amplitude of 2.92, 2.97, 2.32, and 2.89 W/m², respectively. Again, the response of the ground floor thermal bridges reveals their stationary and dynamic characteristics as discussed earlier.



(a)



(b)

Figure 7. Inside wall temperature and heat flux of the thermal bridges of the ground floor using tested four walls. (a) inside wall temperature, (b) inside heat flux.

The presented results under the variable inlet air temperature confirmed the results reported in Section 3.1.1 under the standard indoor and outdoor air temperatures. The EIFS wall type provides the best characteristics for thermal bridges between floors and on the roof whereas the AAC-B wall offers the best for the thermal bridge on the ground floor. However, it is to be noted that the difference between the EIFS and the AAC-B walls in the ground floor thermal bridge is less than 0.4 °C for the average inside wall temperature and 3.1 W/m² for the average inside heat flux. On the other hand, the EIFS is more superior to the AAC-B for the thermal bridges of the roof and intermediate floors. In addition, the EIFS is far suitable for high-rise buildings as they have many intermediate floors, and the AAC-B is better only for the thermal bridge of the ground floor.

3.2. Effect of Insulation Thickness and Location

To analyze the reasons for the excellent performance of the EIFS wall structure, it is subjected to further analysis. Table 1 indicates that both the classical and EIFS walls have the same thermal insulation and the same thickness of 5 cm thick. The only difference between them is that the first has the insulation between the wall layers while the EIFS board has the insulation layer on the outer side. Thus, the EIFS is investigated for different locations (inside or outside layer) and thicknesses (2.5 and 5.0 cm) of thermal insulation for the case of the thermal bridge of intermediate floors. Table 5 lists the stationary and dynamic characteristics of the thermal bridge of intermediate floors for different insulation locations and thicknesses under the standard indoor and outdoor air temperatures. Clearly, the thermal insulation on the outside layer of the wall is very effective as it covers both bricks and concrete slab of the floor and roof whereas the inside layer of the insulation is interrupted at many locations. Thus, the effect of thermal bridge on the buildings with inside insulation is more distinct than buildings with outside insulation. As a result, the thermal resistance for the thermal bridges using the outside continuous insulation layer is considerably larger than those using the inside interrupted insulation layer that never covers the concrete slabs. The thermal bridge characteristics (R , T_i , q_i , and A_i) using external insulation of 2.5 cm are comparable to the characteristics using the inside insulation of 5 cm thick. In addition, as the thickness of either outside or inside thermal insulation increases, the characteristics of the thermal bridge between floors are enhanced (Table 5).

Table 5. Effect of insulation thickness and location of the EIFS walls on the thermal bridge between floors using the standard conditions.

Insulation Position and Thickness	C kJ/m ² K	R m ² K/W	$a \times 10^7$ m ² /s	T_e °C	T_i °C	q_i W/m ²	A_i W/m ²	a_i h
Outside, 2.5 cm	690.04	1.039	7.775	0.958	0.113	0.962	0.197	7.75
Outside, 5.0 cm	690.82	1.667	8.315	0.974	0.071	0.600	0.1101	8.25
Inside, 2.5 cm	669.36	0.811	7.498	0.946	0.139	1.233	0.2907	7.75
Inside, 5.0 cm	678.64	1.033	7.993	0.958	0.106	0.968	0.1865	8.25

In addition, Figure 8a,b show the inside wall temperature and heat flux, respectively, for the four considered cases of external and internal insulation, under the hot climate temperature condition. Again, the inside wall temperature and the heat flux of the intermediate floor thermal bridge with the outside insulation of 2.5 cm thick are comparable with those of the thermal bridge with the inside insulation of 5 cm thick. The thermal bridges between floors with the outside insulation of 5 and 2.5 cm and the inside insulation of 5 and 2.5 cm have average inside wall temperature of 25.1, 25.8, 25.7, and 26.2 °C with an inside heat flux of 9.28, 15.12, 15.40, and 19.62 W/m², respectively. The corresponding inside heat flux amplitudes, of the listed cases, are 3.52, 4.77, 5.70, and 7.61 W/m². In conclusion, the uninterrupted external insulation of 5 cm of the thermal bridge of intermediate floors provides lower inside heat flux by about 66% and heat flux amplitude by about 62% than

the same thermal bridge with interrupted internal insulation. This is mainly due to the larger effect of thermal bridges on the interrupted internal insulation as discussed earlier.

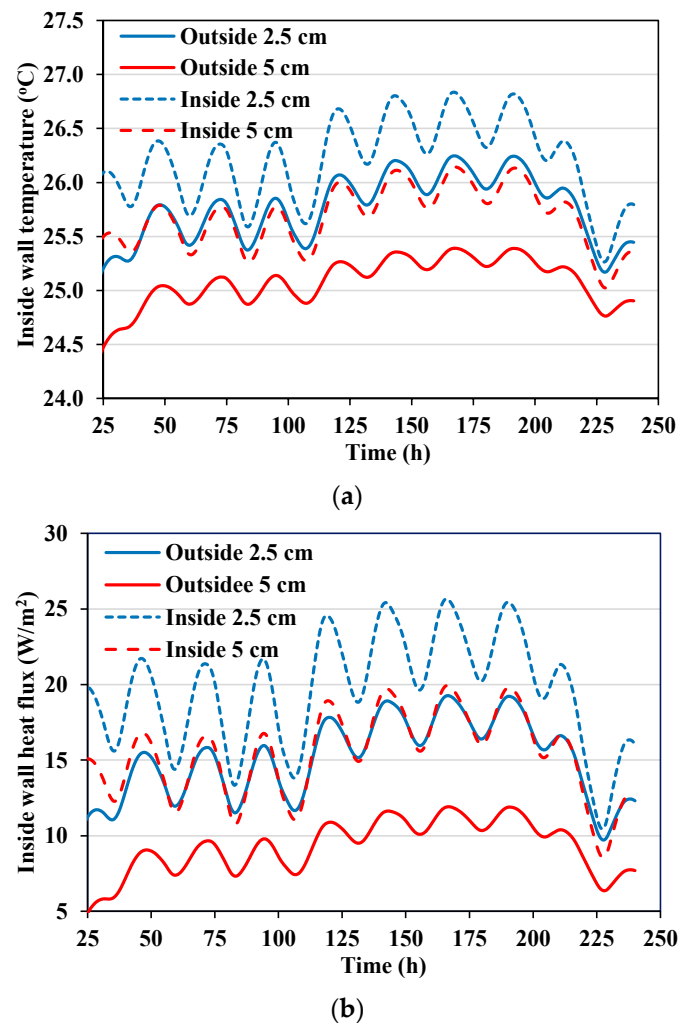


Figure 8. Effect of the insulation thickness and location on the thermal bridge of the intermediate floors using EIFS wall type. (a) inside wall temperature, (b) inside heat flux.

3.3. Thermal Characteristics of the Building Envelope

The building envelopes have thermal bridges at the junctions between walls and columns, concrete slabs of intermediate floors, ground floor, roof, etc. In this paper, the envelope characteristics are identified by the assembly thermal resistance concept that is applied to compare the different wall structures considered in this work.

Figure 9 shows the thermal resistances of the tested four wall structures and their thermal bridge resistances. The thermal bridge of the ground floor slab has higher resistance than the AAC-B and AAC-CB walls and lower resistance than the other wall structures. It is observed that the EIFS is the least influenced wall structure by the effect of the various thermal bridges, i.e., the effect of thermal bridges on the EIFS wall is considerably lower than the other tested walls. The presented resistances, in Figure 9, are implemented in Equations (6)–(11) with their corresponding areas to evaluate the equivalent resistance of the building envelope and the various floors using the tested four wall structures.

Table 6 lists the rate of heat flow per one degree (reciprocal of the total thermal resistance) of the various floors and the building envelope for both tested small room (4 m × 4 m × 4 m) and relatively large building (30 m × 20 m × 4 m). The smaller the value of $Q/\Delta T$ is the better the characteristics of the building envelope and vice versa. For both the small room and large building, the AAC-B wall structure is the best for the

ground floor with a marginal difference from the EIFS wall, whereas the EIFS is the best wall structure for the first and last floors and the whole building. Considerable variations are observed of the resistance between the last floor and the other two floors for all wall structures, particularly for the large building. This is due to the large area of the roof slab relative to the wall area of the last floor of the large building compared to that of the small room. The last line in Table 6 gives the ratio of Q/Q_{EIFS} that reveals the superiority of the EIFS wall over the other wall types, particularly the AAC-CB and classical walls. This is confirmed by the fact that the heat transfer through the building envelope made of either AAC-CB, classical, or AAC-B is higher than that made of EIFS by 102, 51, or 14% for the small room and by 73, 36, or 8% for the large building, respectively.

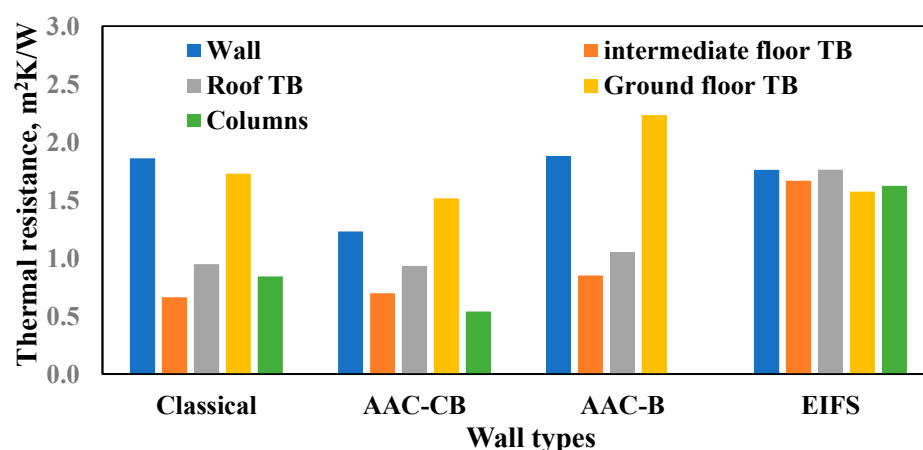


Figure 9. Thermal resistances of the various wall types and thermal bridges using the tested four walls.

Table 6. Rate of heat flow per one degree, $Q/\Delta T$ (W/K), of the small and large buildings for various floors and the building envelope.

Floor	Small Room, Each Floor is $4 \times 4 \times 4 \text{ m}^3$				Large House, Each Floor is $30 \times 20 \times 4 \text{ m}^3$			
	Classical	AAC-CB	AAC-B	EIFS	Classical	AAC-CB	AAC-B	EIFS
Ground	57.259	77.181	38.527	39.573	338.920	458.340	240.80	247.42
First	55.644	74.619	38.720	35.723	331.621	444.825	242.00	222.18
Last	68.807	90.487	59.528	44.772	630.703	757.406	557.37	489.68
Envelope	181.71	242.29	136.77	120.07	1301.24	1660.57	1040.17	959.28
Q/Q_{EIFS}	1.51	2.02	1.14	1.00	1.36	1.73	1.08	1.00

Table 7 provides the resistance per unit area, R_a ($\text{m}^2\text{K}/\text{W}$), of the residential building and its three floors for envelopes made of the tested four wall structures. The AAC-CB wall structure provides the lowest performance (smallest resistance) among all the wall types whereas the EIFS achieves the best performance, except for the ground floor where the AAC-B attains slightly better performance. The resistance of the last floor is larger than those of the other floors by 3–48% for the large building and 0–4% for the small one, except for the AAC-B where the resistance of the last floor is lower than those of the other floors in the case of a small building. This is explained by the fact that the roof has the largest resistance among all components and the large building has a larger roof area (600 m^2) than the small building (16 m^2).

The lower section in Table 7 indicated that the resistances of the classical, AAC-CB, and AAC-B walls are about 0.66, 0.50, and 0.88, respectively, of the resistance of EIFS of the small room. This means that residential houses built using the AAC-CB will have almost double the heat transfer through envelope compared to the buildings of EIFS walls. However, the ratio of the resistance of the large building to that of the small buildings ranges from 1.08 to 1.26, indicating that the size of the building has a quantitative effect on

the thermal effectiveness of the building envelope. Nevertheless, the building size has no qualitative effect on the building effectiveness as the order of the wall types is the same for large and small buildings.

Table 7. Resistance per unit area ($\text{m}^2\text{K}/\text{W}$) of the small and large buildings for various floors and the building envelope.

Floor	Small Room, Each Floor is $4 \times 4 \times 4 \text{ m}^3$				Large House, Each Floor is $30 \times 20 \times 4 \text{ m}^3$			
	Classical	AAC-CB	AAC-B	EIFS	Classical	AAC-CB	AAC-B	EIFS
Ground	1.1826	0.8773	1.7575	1.7111	1.2487	0.9233	1.7575	1.7105
First	1.1502	0.8577	1.6529	1.7916	1.2062	0.8992	1.6529	1.8003
Last	1.1742	0.8929	1.3572	1.8045	1.6033	1.3351	1.8142	2.0650
Envelope	1.1562	0.8660	1.5342	1.7476	1.3921	1.0909	1.7416	1.8882
Walls	1.86	1.23	1.88	1.76	1.86	1.23	1.88	1.76
$R_{\text{envelop}}/R_{\text{walls}}$	0.622	0.704	0.816	0.993	0.748	0.887	0.926	1.073
$(RA)/(RA)_{\text{EIFS}}$	0.6616	0.4955	0.8779	1.0000	0.7372	0.5777	0.9223	1.0000
$(RA)_L/(RA)_S$	1.2040	1.2600	1.1350	1.0800	1.2040	1.2600	1.1350	1.0800

In addition, Table 7 gives the ratio of the building envelope resistance to the wall resistance for the four wall structures. It is clear that the ratio of the envelope resistance to the wall resistance of the EIFS is less than 1% for the small room and 1.07 for the large building. The greater ratio of the resistance of the large building is attributed to the effect of the large roof area, which has the largest thermal resistance.

Figure 10a,b show the overall heat transfer coefficient of the various building structures for the small room and large building, respectively. It ranges from $0.53 \text{ W}/\text{m}^2\text{K}$ for the large building to $0.57 \text{ W}/\text{m}^2\text{K}$ for the small room with an average value of $0.55 \text{ W}/\text{m}^2\text{K}$, for the EIFS residential building envelope. The average overall heat transfer coefficients of AAC-B, classical, and AAC-CB building envelopes are 0.613, 0.792, and $1.036 \text{ W}/\text{m}^2\text{K}$, respectively, with an average increase of 11.5, 44.0, and 88.4% compared to that of the EIFS envelope. This reflects the heat gain/loss increase to/from the residential buildings made of the three listed wall types relative to that made of the EIFS. Therefore, the EIFS wall is the best type recommended for the effective envelope of residential buildings.

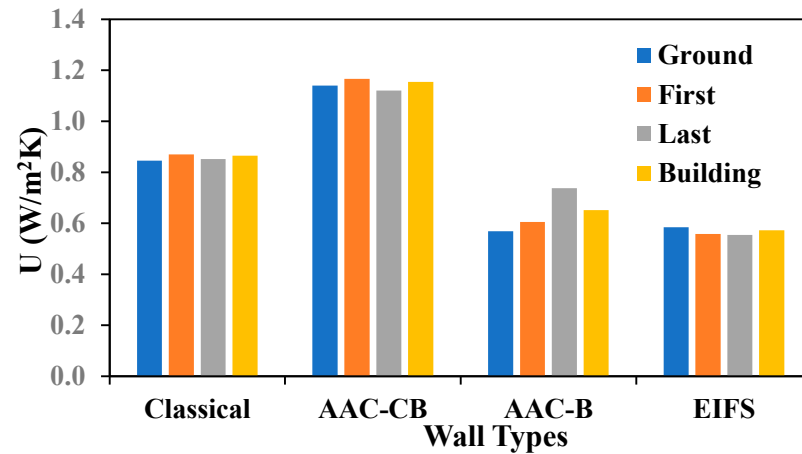
In addition, the effect of wall types is extended to include high-rise buildings by evaluating their overall heat transfer coefficients. Table 8 lists the overall heat transfer coefficients for buildings with 1, 10, 20, 30, 40, and 50 intermediate floors for the three types of the wall structure. It is to be noted that the AAC-B structure is not suitable for high-rise buildings as it does not contain columns for supporting such buildings. The superiority of the EIFS structure is further confirmed for high-rise buildings as the ratio of U/U_{EIFS} increases from 1.36 to 1.48 for classical and from 1.73 to 1.98 for AAC-CB as the number of intermediate floors increases from 1 to 50.

Table 8. Effect of number of intermediate floors on the overall heat transfer coefficient of the high-rise buildings.

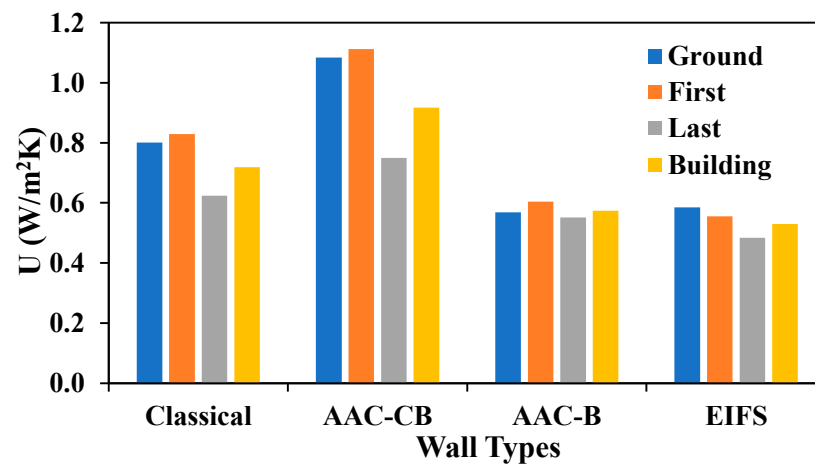
Number of Intermediate Floors	Classical	AAC-CB	AAC-B	EIFS	Classical	AAC-CB	AAC-B	EIFS
	$U \text{ (W}/\text{m}^2\text{K)}$				U/U_{EIFS}			
1	0.71836	0.9167	0.5742	0.5296	1.3564	1.7309	1.0842	
10	0.79200	1.0467	–	0.5468	1.4485	1.914	–	
20	0.80777	1.0745	–	0.5505	1.4674	1.9519	–	
30	0.81411	1.0839	–	0.5520	1.4750	1.9636	–	1.00
40	0.81745	1.0918	–	0.5528	1.4789	1.9750	–	
50	0.81970	1.0955	–	0.5533	1.4816	1.9799	–	

Based on the reported results, the building envelope made using AAC-CB has the lowest performance among the tested wall structures. At the same time, the AAC-CB is

a common practice in many countries of hot climates. The present results showed great concern about that wall type and urge hot climate countries to review their common practice wall structure and replace the AAC-CB with the EIFS wall or at least modify it by adding an external insulation layer covered with suitable cladding material. The return of this replacement will be beneficial on the individual and national levels in terms of energy and environment.



(a)



(b)

Figure 10. (a) Overall heat transfer coefficient of the small room for various floors and the building envelope; (b) Overall heat transfer coefficient of the large building for various floors and the building envelope.

4. Conclusions and Future Work

The effect of wall type on the thermal performance of building envelope in a hot climate is investigated considering the walls, foundation, roof, thermal bridges between columns and walls, and at the junctions between walls and slabs of the ground floor, roof, and intermediate floors. Four wall types that are used in hot climates, namely, classical, autoclaved aerated concrete bearing (AAC-B), AAC column and beam (AAC-CB), and exterior insulation and finish system (EIFS) are tested. Based on the reported results, the following conclusions may be drawn:

The inner heat flux of the thermal bridge using EIFS is lower than that using AAC-CB, classical, and AAC-B walls by 60.2, 58.1, and 49.0%, respectively, for the thermal bridge of the intermediate floors, by 40.1–47.0% for the thermal bridge of the roof, and 30–50% for the thermal bridge of the reinforced concrete column.

The maximum temperatures of classical, AAC-CB, AAC-B, and EIFS thermal bridges of the intermediate floors are damped from 48 °C for the outdoor air temperature to 28.9, 27.2, 26.4, and 25.4 °C while the temperature amplitude is reduced from 19.57 °C to 2.46, 1.92, 1.12, and 0.91 °C, respectively. In addition, the maximum temperature is damped by 21.4–22.6 °C for the thermal bridges of the roof.

The building envelope made of EIFS is the least affected building envelope by the thermal bridges as the ratio of the envelope thermal resistance to its wall resistance is 0.748, 0.887, 0.926, and 1.073 for classical, AAC-CB, AAC-B, and EIFS, respectively. Thus, the thermal bridges have a significant effect on the building envelopes made of classical and AAC-CB walls compared to those made of AAC-B and EIFS walls.

Although the AAC-CB is a common external building structure in hot climates, it has the lowest performance among the tested wall structures. Thus, there is great concern about the AAC-CB wall type and hot climate countries are encouraged to replace the AAC-CB with the EIFS wall or modify it by an external insulation layer with a suitable cladding layer. This replacement will be beneficial on the individual and national levels in terms of energy and environment as the heat exchange with the environment will be reduced by about 51%.

The average overall heat transfer coefficients of EIFS, AAC-B, classical, and AAC-CB building envelopes are 0.55, 0.613, 0.792, and 1.036 W/m²K, respectively. Thus, the average increase of the last three building envelopes over the EIFS envelope is 11.5, 44.0, and 88.4%, respectively.

The uninterrupted insulation at the exterior layer of the wall that covers both wall and concrete slabs attains an effective building envelope and prevents a considerable amount of heat loss that bypasses the discontinuous insulation layer elsewhere. The thermal bridge with external insulation of 5cm provides inside heat flux and heat flux amplitude lower than the same thermal bridge with an internal insulation layer of the same thickness by about 66 and 62%, respectively.

The EIFS wall provides an efficient building envelope that reduces the heat exchange with the outdoor environment for residential buildings by 101.8, 51.2, and 13.9% than the AAC-CB, AAC-B, and classical walls, respectively.

The overall heat transfer coefficient for a small building is larger than that for a large building by 8, 13.5, 20.4, and 26% for the EIFS, AAC-B, classical, and AAC-CB walls, respectively.

As the number of intermediate floors increases from 1 to 50, the overall heat transfer coefficient of the building envelope increases by 4.5, 14.1, and 19.5% for the EIFS, classical, and AAC-CB walls, respectively.

The present work focuses on the thermal performance of the building envelopes using four different wall types, considering the total thermal resistance and the overall heat transfer coefficient. However, the effect of the building envelopes on the cooling load and energy consumption needs to be investigated. This can provide a quantitative effect of the wall types on the energy consumption on residential sector and national levels.

Author Contributions: Conceptualization, A.A. and H.A.-Z.; methodology, H.A.-A. and H.A.-Z.; analysis, validation: H.A.-A. and H.A.-Z.; resources, A.A.; formal analysis, H.A.-A., A.A. and H.A.-Z.; writing—original draft preparation, H.A.-A., A.A. and H.A.-Z.; writing—review and editing, H.A.-A., A.A. and H.A.-Z.; funding acquisition and administration, H.A.-A. All authors have read and agreed to the published version of the manuscript.

Funding: The Public Authority for Applied Education and Training (PAAET), project TS-21-16.

Institutional Review Board Statement: Not applicable.

Informed Consent Statement: Not applicable.

Data Availability Statement: This statement is excluded.

12. Huang, H.; Zhou, Y.; Huang, R.; Wu, H.; Sun, Y.; Huang, G.; Xu, T. Optimum insulation thicknesses and energy conservation of building thermal insulation materials in Chinese zone of humid subtropical climate. *Sustain. Cities Soc.* **2020**, *52*, 101840. [[CrossRef](#)]
13. Al-Sanea, S.; Zedan, M. Improving thermal performance of building walls by optimizing insulation layer distribution and thickness for same thermal mass. *Appl. Energy* **2011**, *88*, 3113–3124. [[CrossRef](#)]
14. Ozel, M. Cost analysis for optimum thicknesses and environmental impacts of different insulation materials. *Energy Build.* **2012**, *49*, 552–559. [[CrossRef](#)]
15. Durakovic, B.; Yildiz, G.; Yahia, M. Comparative performance evaluation of conventional and renewable thermal insulation materials used in building. *Tech. Gaz.* **2020**, *27*, 283–289.
16. Hudobivnik, B.; Pajek, L.; Kunič, R.; Košir, M. FEM thermal performance analysis of multi-layer external walls during typical summer conditions considering high intensity passive cooling. *Appl. Energy* **2016**, *178*, 363–375. [[CrossRef](#)]
17. ISO 14683; Thermal Bridges in Building Construction—Linear Thermal Transmittance—Simplified Methods and Default Values. DIN Deutsches Institut für Normung e. V., Berlin. Beuth Verlag GmbH: Berlin, Germany, 2017.
18. Friess, W.; Rakhshan, K.; Hendawi, T.; Tajerzadeh, S. Wall insulation measures for residential villas in Dubai: A case study in energy efficiency. *Energy Build.* **2012**, *44*, 26–32. [[CrossRef](#)]
19. Hua, G.; Fuad, B. Effect of dynamic modeling of thermal bridges on the energy performance of residential buildings with high thermal mass for cold climates. *Sustain. Cities Soc.* **2017**, *34*, 250–263. [[CrossRef](#)]
20. Hua, G.; Fuad, B. Dynamic effect of thermal bridges on the energy performance of a low-rise residential building. *Energy Build.* **2015**, *105*, 106–118. [[CrossRef](#)]
21. Martin, K.; Martin-Sven, K.; Paul, K.; Karl-Villem, V.; Raimo, S.; Henri, S.; Martin, T.; Jarek, K. PCSP’s Diagonal Tie Connectors Thermal Bridges Impact on Energy Performance and Operational Cost: Case Study of a High-Rise Residential Building in Estonia. *E3S Web Conf.* **2020**, *172*, 08006. [[CrossRef](#)]
22. Zaccaro, F.; Littlewood, J.R.; Hayles, C. An Analysis of Repeating Thermal Bridges from Timber Frame Fraction in Closed Panel Timber Frame Walls: A Case Study from Wales, UK. *Energies* **2021**, *14*, 1211. [[CrossRef](#)]
23. Berggren, B.; Wall, M. State of Knowledge of Thermal Bridges—A Follow up in Sweden and a Review of Recent Research. *Buildings* **2018**, *8*, 154. [[CrossRef](#)]
24. Roberto, G.; Alberto, R.; Daniel, C. Disaggregation process for dynamic multidimensional heat flux in building simulation. *Energy Build.* **2017**, *148*, 298–310. [[CrossRef](#)]
25. Kim, H.; Yeo, M. Thermal Bridge Modeling and a Dynamic Analysis Method Using the Analogy of a Steady-State Thermal Bridge Analysis and System Identification Process for Building Energy Simulation: Methodology and Validation. *Energies* **2020**, *13*, 4422. [[CrossRef](#)]
26. ISO 10211; Thermal Bridges in Building Construction—Heat Flows and Surface Temperatures—Detailed Calculations. DIN-Deutsches Institut für Normung e. V., Berlin. Beuth Verlag GmbH: Berlin, Germany, 2017.
27. Quinten, J.; Feldheim, V. Dynamic modelling of multidimensional thermal bridges in building envelopes: Review of existing methods, application and new mixed method. *Energy Build.* **2016**, *110*, 284–293. [[CrossRef](#)]
28. Quinten, J.; Feldheim, V. Mixed equivalent wall method for dynamic modelling of thermal bridges: Application to 2-D details of building envelope. *Energy Build.* **2019**, *183*, 697–712. [[CrossRef](#)]
29. COMSOL AB. *COMSOL Multiphysics® v. 5.4, Module User’s Guide*; COMSOL AB: Stockholm, Sweden, 2018; pp. 75–84.
30. Paola, G.; Luca, E.; Claudia, G. Description of multilayer walls by means of equivalent homogeneous models. *Int. Commun. Heat Mass Transf.* **2018**, *91*, 30–39. [[CrossRef](#)]